Glutathione-Triggered Disassembly of Dual Disulfide Located Degradable Nanocarriers of Polylactide-Based Block Copolymers for Rapid Drug Release

ARTICLE *in* BIOMACROMOLECULES · JULY 2014

Impact Factor: 5.75 · DOI: 10.1021/bm5008508 · Source: PubMed

2 AUTHORS:

Na Re Ko
Kyung Hee University
10 PUBLICATIONS **181** CITATIONS
SEE PROFILE

Jung Kwon Oh
Concordia University Montreal
78 PUBLICATIONS **3,474** CITATIONS
SEE PROFILE

Article

pubs.acs.org/Biomac

Glutathione-Triggered Disassembly of Dual Disulfide Located Degradable Nanocarriers of Polylactide-Based Block Copolymers for Rapid Drug Release

Na Re Ko and Jung Kwon Oh*

Department of Chemistry and Biochemistry and Center for Nanoscience Research, Concordia University, Montreal, Quebec Canada H4B 1R6

Supporting Information

ABSTRACT: Reduction-responsive degradation based on disulfide-thiol chemistry is highly desirable in the development of self-assembled block copolymer nanocarriers for multifunctional polymer-based drug delivery applications. Most conventional approaches involve the incorporation of disulfide linkages at a single location. Herein, we report a new dual disulfide located degradable polylactide (PLA)-based block copolymer (DL-ssABP) synthesized by a combination of ring opening polymerization, facile coupling reactions, and controlled radical polymerization. The amphiphilic design of the DL-ssABP enables the formation of self-assembled micelles having disulfides positioned both in the hydrophobic PLA core and at the core/corona interface. The reductive response to glutathione as a cellular trigger results in the cleavage of the disulfide linkage at the interface shedding hydrophilic coronas as well as the disulfides in the PLA core causing disintegration of PLA cores. Such dual disulfide degradation process leads to a synergistically enhanced release of encapsulated anticancer drugs in cellular environments. These results, combined with flow cytometry and confocal laser scanning microscopy (CLSM) as well as cell viability measurements, suggest that DL-ssABP offers versatility in tumor-targeting controlled/enhanced drug delivery applications.

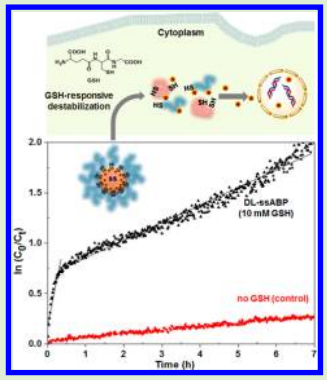

INTRODUCTION

Polymer-based drug delivery systems, particularly self-assembled micelles based on block copolymers have drawn significant attention as promising candidates for tumor-targeting drug delivery applications.[1−5] Well-defined micellar nanocarriers having optimal sizes (50−150 nm in diameter) can minimize renal clearance by kidney filtration as well as prevent their extravasation into healthy cells, common to small drugs. The nanocarriers formulated with hydrophilic neutral surface coatings exhibit a prolonged blood circulation.[6−8] Tumors are characterized with rapidly grown vasculatures with irregularly aligned endothelial cells which facilitates extravasation (enhanced permeation) of drug-carrying micelles into tumors. Furthermore, their insufficient lymphatic drainage allows for these micelles to be retained inside solid tumors (retention). This process is known as the enhanced permeation and retention (EPR) effect (or passive targeting).[9−11] These features offer micellar nanocarriers to minimize undesired side effects and maximize drug efficacy. Once internalized into cancer cells through endocytosis, nanocarriers undergo sustainable release of anticancer drugs inside cells.[12,13]

A classical model of drug release involves a diffusion-controlled mechanism which requires overcoming hydrophobic−hydrophobic interactions between drug molecules and micellar core-forming polymers. This mechanism is facile, but uncontrolled and slow.[14] A promising method is the incorporation of dynamic covalent bonds (i.e., cleavable linkages) in the design and development of block copolymers and their nanostructures. When needed, the cleavable linkages are cleaved in response to external stimuli, causing degradation or destabilization of the micelles. This stimuli-responsive degradation (SRD) can enhance the release of encapsulated drugs as well as facilitate the removal of empty vehicles after drug release.[15−18] Several stimuli-responsive cleavable linkages have been explored, including acid-labile,[19,20] photocleavable groups,[21−23] and polypeptides.[24] In particular, disulfides are cleaved to the corresponding thiols in response to reductive reactions.[25,26] In biological systems, glutathione (GSH, a tripeptide containing cysteine having a pendant thiol) is found at millimolar concentrations (2−10 mM) in intracellular compartments, while its concentration is much smaller in extracellular milieu (<10 μM). Such large redox potential between intracellular and extracellular compartments as well as enhanced concentration in cancer cells renders GSH an effective cellular trigger that can cleave disulfide linkages in micellar nanocarriers through disulfide-thiol exchange reactions.[27,28] Due to these features, block copolymer based micelles exhibiting redox-responsive degradation have been considered as a promising platform for tumor-targeting drug delivery applications.[29−31]

Several approaches have been reported for the synthesis of disulfide-containing block copolymers and their self-assembled

Received: June 10, 2014
Revised: July 11, 2014
Published: July 15, 2014

Scheme 1. Preparation and Illustration of a Dual Location Disulfide Degradable DL-ssABP [POEOMA-ss-(PLA-ss-PLA)-ss-POEOMA] Triblock Copolymer, and Its Self-Assembled Doxorubicin-Loaded Micelles as Effective Intracellular Drug Delivery Nanocarriers

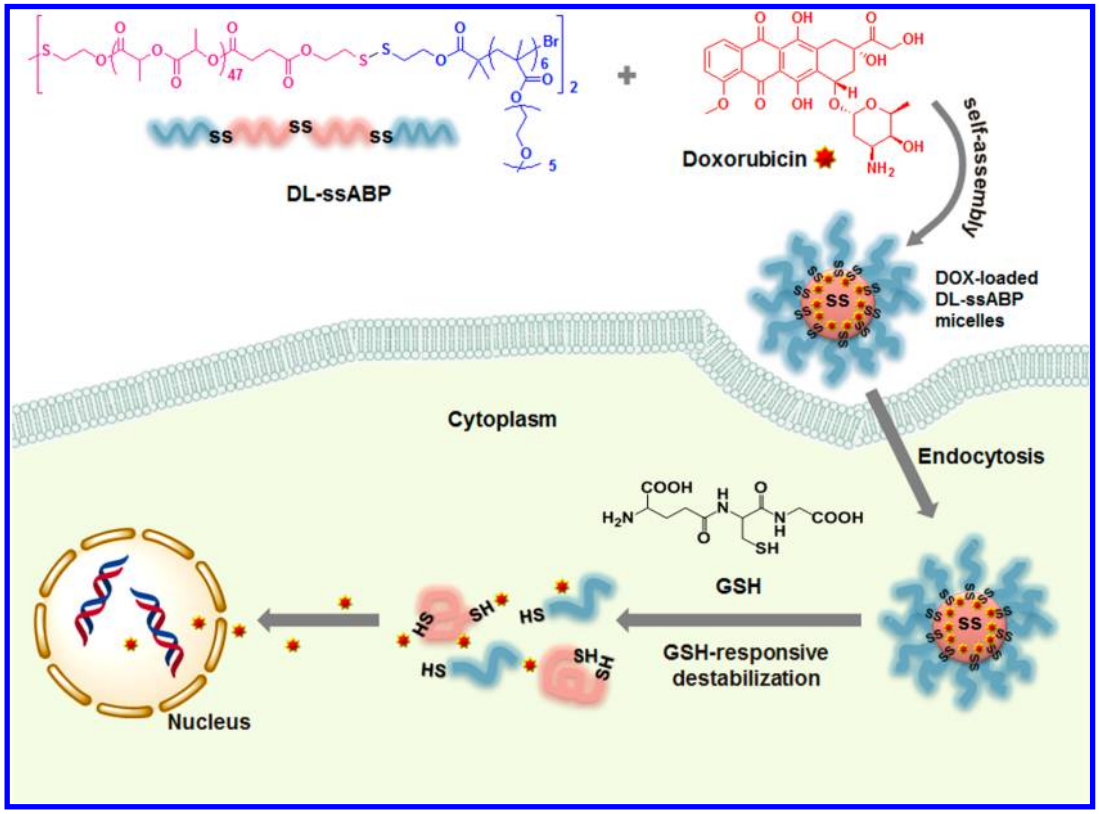

nanostructures. Most approaches involve the incorporation of different densities of disulfide linkages positioned at a single location, either in backbone of the polymer chains as single[32−36] and multiple groups,[37−42] as pendant chains,[43−46] as cross-linkers,[47−54] or at block junctions.[55−67] A new multilocation SRD strategy has recently been explored to develop effective reduction-responsive nanocarriers. They possess disulfide linkages in dual locations, namely in the micellar core, in interlayered corona, and at the interface between hydrophobic core and corona. The preliminary results suggest that this strategy enables the accelerated release of encapsulated anticancer drugs in response to reductive reductions at both sites.[68,69]

In this work, we have explored the promising multilocation SRD strategy to develop novel dual location disulfide degradable polylactide (PLA)-based block copolymers (DL-ssABPs) and their self-assembled micelles as effective intracellular drug delivery nanocarriers exhibiting rapid reduction-responsive drug release. Compared to hydrophobic polymethacrylate-containing pendant disulfide linkages,[69] PLA is a typical class of aliphatic polyesters and is biocompatible, biodegradable by hydrolysis and enzymatic reactions, and FDA-approved for clinical use.[70−72] As illustrated in Scheme 1, the DL-ssABP triblock copolymer consists of a hydrophobic central PLA block and hydrophilic polymethacrylate blocks containing pendant oligo(ethylene oxide) (POEOMA). The copolymer has a disulfide bond positioned in the center of the hydrophobic block and two disulfide linkages located at block junctions, thus POEOMA-ss-(PLA-ss-PLA)-ss-POEOMA triblock copolymer. The DL-ssABP self-assembled to form colloidally stable micelles having disulfides located both in the hydrophobic PLA core and at the PLA/POEOMA interface. These disulfide linkages were cleaved in response to GSH (a cellular trigger), shedding the POEOMA coronas from the PLA cores as well as causing disintegration of the PLA cores. The degradation of DL-ssABP micelles enabled the enhanced release of encapsulated anticancer drugs. The results from flow cytometry and confocal laser scanning microscopy (CLSM) as well as cell viability measurements indicate that rapid DOX release from DOX-loaded micelles triggered by higher intracellular GSH concentration resulted in enhanced inhibition of the cellular proliferation.

EXPERIMENTAL SECTION

Instrumentation. ^{1}H NMR spectra were recorded using a 500 MHz Varian spectrometer. The $CDCl_3$ singlet at 7.26 ppm was selected as the reference standard. Molecular weight and molecular weight distribution were determined by gel permeation chromatography (GPC). An Agilent GPC was equipped with a 1260 Infinity Isocratic Pump and a RI detector. Two Agilent PLgel mixed-C and mixed-D columns were used with dimethylformamide (DMF) containing 0.1 mol % LiBr at 50 °C at a flow rate of 1.0 mL/min. Linear poly(methyl methacrylate) standards from Fluka were used for calibration. Aliquots of the polymer samples were dissolved in DMF/LiBr. The clear solutions were filtered using a 0.25 μm polytetrafluoroethylene (PTFE) filter to remove any solvent-insoluble species. A drop of anisole was added as a flow rate marker. Carboxylation, esterification, and monomer conversion were determined using ^{1}H NMR. The size of micelles in hydrodynamic diameter by volume was measured by dynamic light scattering (DLS) at a fixed scattering angle of 175° at 25 °C with a Malvern Instruments Nano S ZEN1600 equipped with a 633 nm He−Ne gas laser. Fluorescence spectra on a Varian Cary Eclipse Fluorescence spectrometer and UV/vis spectra on

dx.doi.org/10.1021/bm5008508 | Biomacromolecules 2014, 15, 3180−3189

an Agilent Cary 60 UV/vis spectrometer were recorded using a 1 cm wide quartz cuvette.

Transmission Electron Microscopy (TEM). TEM images were obtained using a Philips Tecnai 12 TEM, operated at 120 kV and equipped with a thermionic LaB6 filament. An AMT V601 DVC camera with point to point resolution and line resolution of 0.34 and 0.20 nm, respectively, was used to capture images at 2048 by 2048 pixels. To prepare specimens, the micellar dispersions were dropped onto copper TEM grids (400 mesh, carbon coated), blotted, and then allowed to air-dry at room temperature.

Materials. 3,6-Dimethyl-1,4-dioxane-2,5-dione (DL-lactide, LA), 2-hydroxyethyl disulfide (ss-DOH), tin(II) 2-ethylhexanoate ($Sn(Oct)_2$, 95%), succinic anhydride (SA, 99%), triethylamine (Et_3N), *N*,*N*′-dicyclohexylcarbodiimide (DCC), 4-(*N*,*N*-dimethylamino)pyridine (DMAP), copper(I) bromide (CuBr, >99.99%), *N*,*N*,*N*′,*N*″,*N*″-pentamethyldiethylenetriamine (PMDETA, >98%), GSH (a reduced form), Nile Red (NR), and doxorubicin hydrochloride (DOX, $-NH_3^+Cl^-$ forms, >98%) from Aldrich and DL-dithiothreitol (DTT, 99%) from Acros Organics were purchased and used as received. Oligo(ethylene oxide) monomethyl ether methacrylate (OEOMA) with MW = 300 g/mol and pendent EO units ≈ 5 was purchased from Aldrich and was purified by passing through a column filled with basic alumina to remove the inhibitors. 2-Hydroxyethyl-2′-(bromoisobutyryl)ethyl disulfide (HO-ss-iBuBr) was synthesized according to our previous publication.[73]

Synthesis of ss(PLA−OH)$_2$. ss-DOH (0.11 g, 0.69 mmol), LA (10.0 g, 69.4 mmol), $Sn(Oct)_2$ (19.7 mg, 0.05 mmol), and toluene (6.7 mL) were added to a 10 mL Schlenk flask. The resulting mixture was deoxygenated by four freeze−pump−thaw cycles. The reaction flask was filled with nitrogen, thawed, and then immersed in an oil bath preheated at 120 °C to start the polymerization. After 2.5 h, the polymerization was stopped and cooled to room temperature. The resulting homopolymers were precipitated from cold MeOH (note that LA is soluble in MeOH). They were then isolated by vacuum filtration and further dried in a vacuum oven at room temperature overnight, resulting in a white solid. Molecular weight (GPC-DMF/LiBr): M_n = 20 400 g/mol and M_w/M_n = 1.10.

Carboxylation to ss(PLA-COOH)$_2$. A clear solution consisting of the purified, dried ss(PLA−OH)$_2$ (2.5 g, 0.17 mmol) and Et_3N (1.04 g, 8.53 mmol) in anhydrous tetrahydrofuran (THF, 40 mL) was mixed with a solution of succinic anhydride (0.85 g, 8.53 mmol) in THF (10 mL) at 0 °C and then kept at room temperature for 12 h. The reaction mixture was filtered to remove the white solids that formed, then the resulting homopolymers were purified by precipitation from 0.1 M aqueous HCl solution.

Esterification to ss(PLA-ss-Br)$_2$. A mixture of ss(PLA-COOH)$_2$ (1.0 g, 71.9 μmol), HO-ss-iBuBr (65 mg, 0.22 mmol), DMAP (8.79 mg, 71.9 μmol), and dichloromethane (DCM, 9 mL) was mixed with a solution of DCC (0.16 g, 0.79 mmol) in DCM (1 mL) and stirred at room temperature for 12 h. The *N*,*N*′-dicyclohexylurea (DCU) that formed as a byproduct was removed by vacuum filtration. Solvent was evaporated, and the product was purified by precipitation from cold MeOH. The resulting white solids were dried in a vacuum oven at 35 °C for 15 h.

Synthesis of DL-ssABP. ss(PLA-ss-Br)$_2$ (0.5 g, 0.036 mmol), OEOMA (0.22 g, 0.73 mmol), PMDETA (3.8 μL, 0.03 mmol), and THF (0.69 mL) were added to a 10 mL Schlenk flask. The resulting mixture was deoxygenated by three freeze−pump thaw cycles. The reaction flask was filled with nitrogen and CuBr (2.6 mg, 0.02 mmol) was added to the frozen solution. The flask was sealed, purged with vacuum, and backfilled with nitrogen once. The mixture was thawed, and the flask was then immersed in an oil bath preheated to 47 °C to start the polymerization. After 2 h, the polymerization was stopped by cooling and exposing the reaction mixture to air.

For purification, the as-prepared polymer solution was diluted with THF and passed through a basic alumina column to remove residual copper species. The solvent was removed under rotary evaporation at room temperature, and the polymer was isolated by precipitation from hexane, then dried under vacuum at room temperature for 15 h.

Reductive Cleavage of Disulfide Linkages of DL-ssABP in DMF. An aliquot of the dried, purified DL-ssABP (50 mg) was mixed with DTT (2.1 mg, 13.4 μmol) in DMF (10 mL) under stirring at room temperature. Aliquots were taken periodically to analyze molecular weight distribution of degraded products using GPC.

Aqueous Micellization of DL-ssABP Using the Solvent Evaporation Method. Water (10 mL) was added dropwise to a solution consisting of the purified, dried DL-ssABP (12.5 mg) dissolved in THF (1 mL). The resulting dispersion was stirred at room temperature for 24 h to form colloidally stable micellar aggregates in aqueous solution at 1.2 mg/mL.

Determination of Critical Micellar Concentration (CMC) Using a Nile Red (NR) Probe. A stock solution of Nile Red (NR) in THF at 1 mg/mL and a stock solution of DL-ssABP in THF at 1 mg/mL were prepared. Water (10 mL) was added dropwise into a series of mixtures consisting of the same amount of the stock solution of NR (0.5 mL, 0.5 mg NR) and various amounts of the stock solution of DL-ssABP in 20 mL vials. The resulting dispersions were stirred for 24 h to evaporate THF. The dispersions were then filtered using 0.45 μm PES filters to remove excess NR. A series of NR-loaded micelles at various concentrations of DL-ssABP ranging from 5×10^{-6} to 0.4 mg/mL were formed. Their fluorescence spectra were recorded at λ_{max} = 600 nm.

Reductive-Destabilization of Aqueous DL-ssABP Micelles. Aliquots of aqueous micellar dispersion (1.2 mg/mL, 2 mL) were mixed with 10 mM GSH (6.1 mg, 20 μmol) under stirring. Aliquots were taken periodically to follow a change in size distribution by DLS.

Preparation of DOX-Loaded Micelles. Water (10 mL) was dropwise added to a solution consisting of the purified, dried DL-ssABP (20 mg), DOX (2 mg), and Et_3N (1.44 μL, 3 mol equiv to DOX) in DMF (2 mL). The resulting dispersion was transferred into a dialysis tube (MWCO = 3500 g/mol) and dialyzed over water (800 mL) for 48 h, yielding DOX-loaded micelles in water at 1.1 mg/mL. To determine the loading level of DOX, aliquots of the DOX-loaded micellar dispersion (1 mL) were mixed with DMF (5 mL) and their UV/vis spectra were recorded at λ_{ex} = 480 nm. DOX loading was calculated by the weight ratio of loaded DOX to dried polymers.

GSH-Triggered Release of DOX from Aqueous DOX-Loaded Micelles. An aliquot of DOX-loaded micellar dispersion (3 mL, 1.1 mg/mL) was transferred into a dialysis tubing (MWCO = 12 000 g/mol) and immersed in aqueous phosphate-buffered saline (PBS) solution (50 mL) as a control and 10 mM aqueous GSH buffered with PBS solution under stirring. The absorbance of DOX in outer water (50 mL) was recorded at 2 min interval using a UV/vis spectrometer equipped with an external probe at λ = 497 nm. For quantitative analysis, DOX (38.9 μg, equivalent to DOX encapsulated in 3 mL DOX-loaded micelles) was dissolved in 10 mM aqueous GSH buffered with PBS solution (50 mL), and its UV/vis spectrum was recorded.

Cell Culture. HeLa cancer cells were cultured in Dulbecco's modified Eagle's medium (DMEM) containing 10% fetal bovine serum (FBS) and 1% antibiotics (50 units/mL penicillin and 50 units/mL streptomycin) at 37 °C in a humidified atmosphere containing 5% CO_2.

Flow Cytometry. HeLa cells were plated at 5×10^5 cells/well into a six-well plate and incubated in DMEM (2 mL) at 37 °C. After 24 h, cells were treated with DOX-loaded DL-ssABP micelles (223.9 μL, DOX = 2.2 μg/mL) at 37 °C for 16 h. After the culture medium was removed, the cells were washed with PBS solution and treated with trypsin. The cells were suspended in DMEM (500 μL) for flow cytometry measurements. Data analysis was performed by means of a BD FACSCANTO II flow cytometer and BD FACSDiva software.

Confocal Laser Scanning Microscopy (CLSM). HeLa cells plated at 2×10^5 cells/well into a 6-well plate and incubated for 24 h in DMEM (2 mL) were treated with DOX-loaded micelles (DOX = 2.2 μg/mL) at 37 °C for 16 h. After culture medium was removed, cells were washed with PBS buffer three times. After the removal of supernatants, the cells were fixed with cold methanol (−20 °C) for 20 min at 4 °C. The slides were rinsed five times with PBS solution and three times with TBST (tris-buffered saline Tween-20). Cells were stained with 2-(4-amidinophenl)-6-indolecarbamidine (DAPI). The

Scheme 2. Synthesis of a Reduction-Responsive Dual Location Disulfide Degradable DL-ssABP Triblock Copolymer by a Combination of Ring Opening Polymerization, Coupling Reactions, and Atom Transfer Radical Polymerization

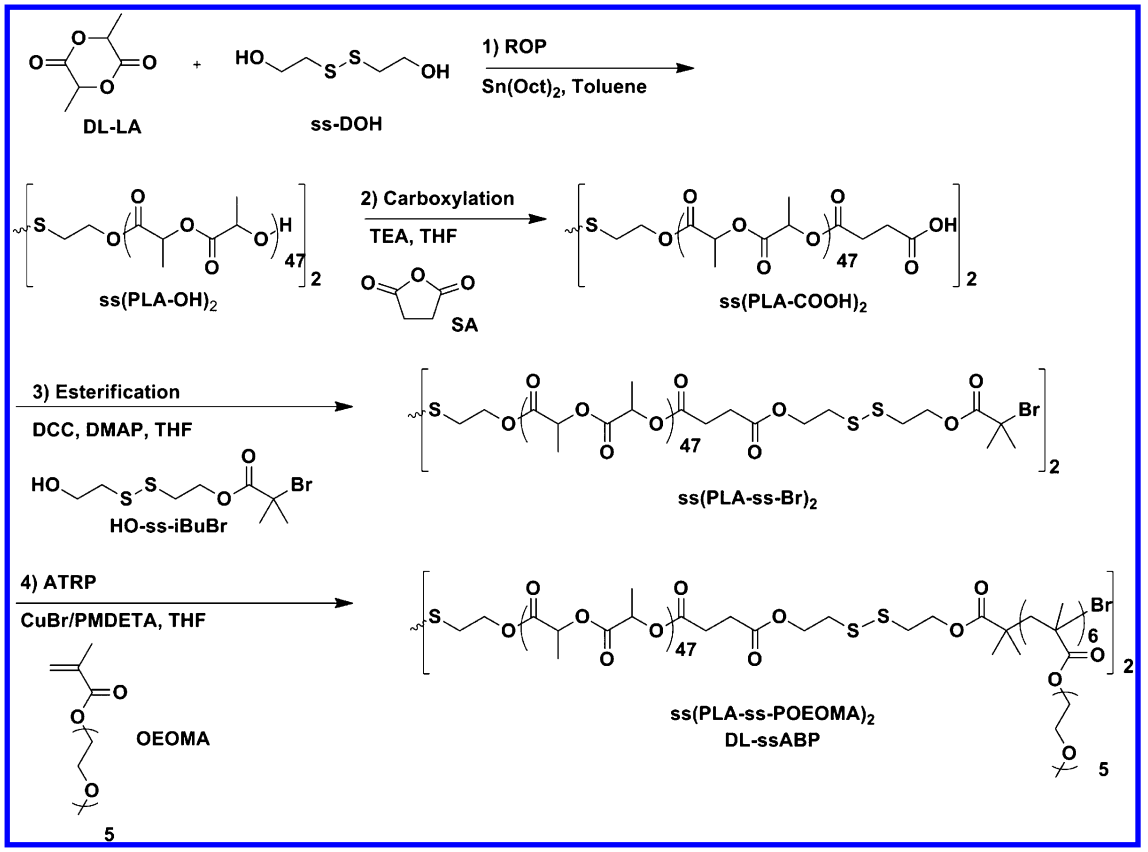

fluorescence images were obtained using a LSM 510 Meta/Axiovert 200 (Carl Zeiss, Jena, Germany).

Cell Viability Using MTT Assay. HeLa cells were plated at 5×10^5 cells per well into a 96-well plate and incubated for 24 h in DMEM (100 μL) containing 10% FBS and 1% antibiotics. Then, they were incubated with various concentrations of empty (DOX-free), free DOX, and DOX-loaded micelles of DL-ssABP for 48 h. Blank controls without micelles (cells only) were run simultaneously as a control. Cell viability was measured using CellTiter 96 Non-Radioactive Cell Proliferation Assay kit (MTT, Promega) according to the manufacturer's protocol. Briefly, 3-(4,5-dimethylthiazol-2-yl)-2,5-diphenyltetrazolium bromide (MTT) solutions (15 μL) was added into each well. After 4 h incubation, the medium containing unreacted MTT was carefully removed. Dimethyl sulfoxide (DMSO;100 μL) was added into each well in order to dissolve the formed formazan purple crystals, and then the absorbance at λ = 570 nm was recorded using Powerwave HT Microplate Reader (Bio-Tek). Each concentration was 12-replicated. Cell viability was calculated as the percent ratio of absorbance of mixtures with micelles to control (cells only).

RESULTS AND DISCUSSION

Synthesis and Reduction-Responsive Degradation of DL-ssABP. Scheme 2 illustrates our approach to synthesize POEOMA-ss(PLA-ss-PLA)-ss-POEOMA having disulfide linkages positioned both in the center of triblock copolymer and at the block junctions.

The first step is the synthesis of well-controlled ss(PLA–OH)$_2$ by ring opening polymerization (ROP) of LA initiated with ss-DOH at 120 °C in toluene. The detailed procedure is described in our previous report.[33] Here, the resulting ss(PLA–OH)$_2$ had a number-average molecular weight, M_n = 20 400 g/mol with M_w/M_n = 1.10 determined by GPC (Figure S1) and a degree of polymerization (DP) = 94 determined by ^{1}H NMR (Figure 1a). The second step is the carboxylation of ss(PLA–OH)$_2$ with excess SA in anhydrous THF, converting the ss(PLA–OH)$_2$ to ss(PLA-COOH)$_2$. ^{1}H NMR was used to follow the conversion. As seen in Figure 1b, the multiplet at 4.3–4.4 ppm (e) corresponding to terminal methine protons in the backbone of PLA chains disappeared, while the peaks at 2.6–2.8 ppm (f,g), corresponding to methylene protons of succinic moiety, appeared as a consequence of the carboxylation. From the integral ratio of peaks [(b/2)/{(f+g)/4}], the conversion was calculated to be >95%. The third step is the esterification of the purified, dried ss(PLA-COOH)$_2$ by a facile carbodiimide coupling reaction with a double-head initiator (HO-ss-iBuBr), yielding a brominated ss(PLA-ss-Br)$_2$. As seen in Figure 1c, a singlet at 1.95 ppm (l) corresponding to six methyl protons in terminal iBuBr moieties appeared as a result of the successful bromination. From the integral ratio of peaks [(b/2)/(l/6)], the conversion was also calculated to be >98%.

The last step is the chain extension of ss(PLA-ss-Br)$_2$ with water-soluble POEOMA using atom transfer radical polymerization (ATRP).[74,75] The ATRP conditions include [OEOMA]$_0$/[ss(PLA-ss-Br)$_2$]$_0$/[CuBr/PMDETA]$_0$ = 20/1/0.5 in THF at 47 °C. After 2 h, conversion from OEOMA to POEOMA was determined to be 60% using ^{1}H NMR. The resulting DL-ssABP triblock copolymer had M_n =26 400 g/mol with M_w/M_n = 1.13 by GPC (Figure S1). ^{1}H NMR indicates the DP of POEOMA block = 12 calculated from the integral ratio of the peaks [(b/2)/(m/3)] (Figure 2). These results suggest the successful synthesis of well-defined POEOMA$_6$-ss-(PLA$_{47}$-ss-PLA$_{47}$)-ss-POEOMA$_6$ triblock copolymers with

dx.doi.org/10.1021/bm5008508 | Biomacromolecules 2014, 15, 3180–3189

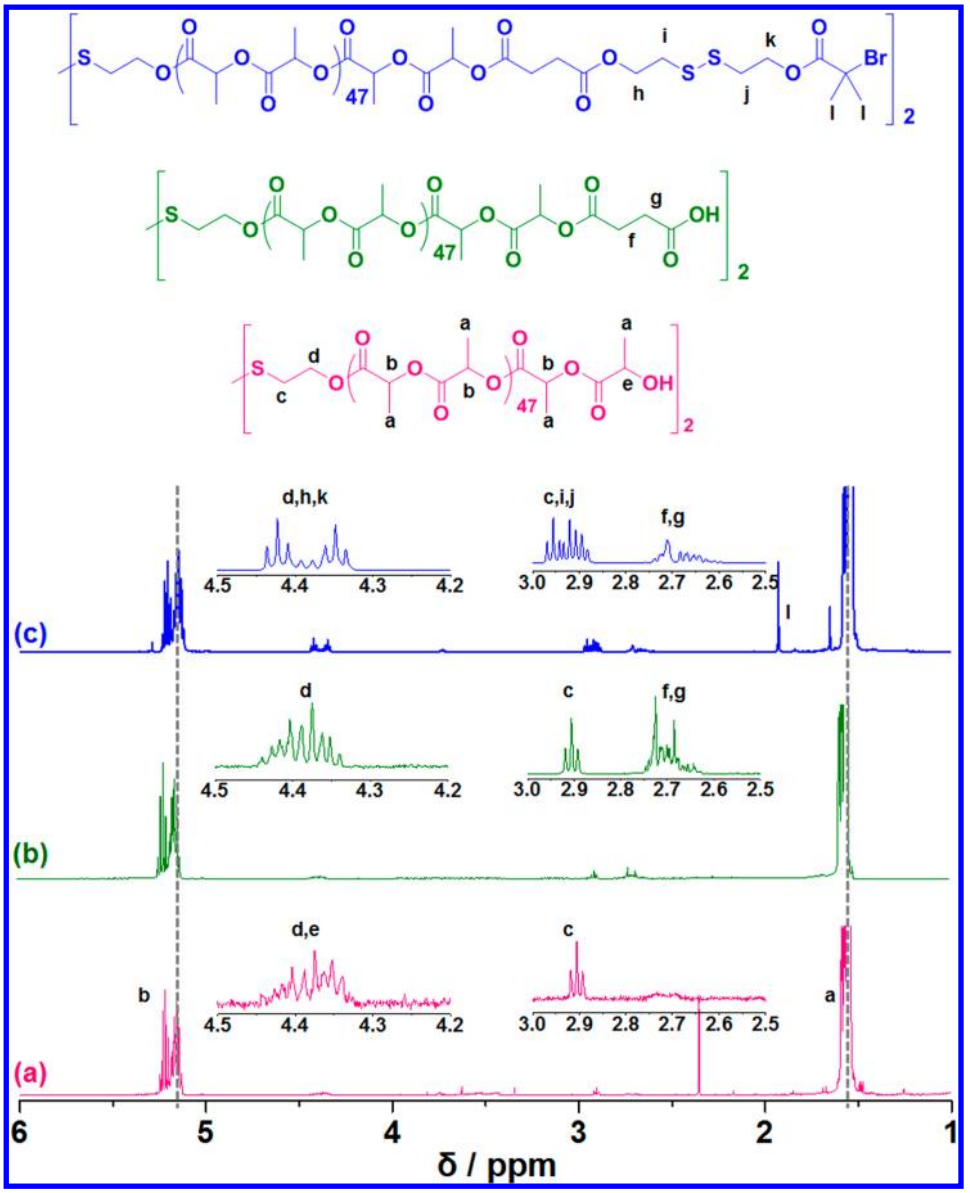

Figure 1. ^{1}H NMR spectra of ss(PLA−OH)$_2$ (a), ss(PLA-COOH)$_2$ (b), and ss(PLA-ss-Br)$_2$ (c) in $CDCl_3$.

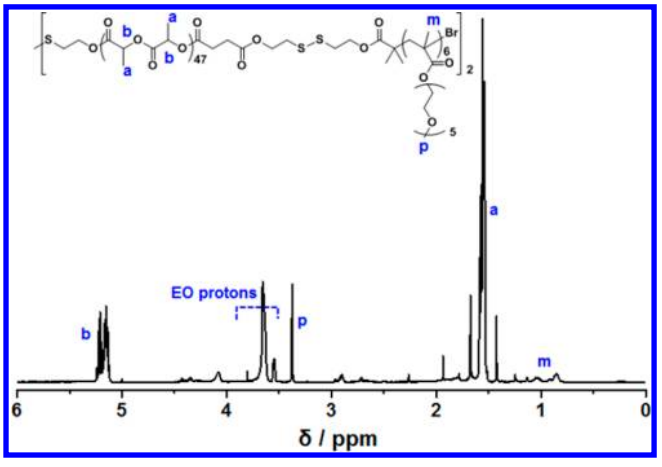

Figure 2. ^{1}H NMR spectrum of DL-ssABP in $CDCl_3$. Conditions for ATRP: $[OEOMA]_0/[ss(PLA\text{-}ss\text{-}Br)_2]_0/[CuBr/PMDETA]_0$ = 20/1/0.5; OEOMA/THF = 0.4/1 wt/wt in THF at 47 °C.

disulfide linkages in the center of the hydrophobic block and at block junctions.

The resulting DL-ssABP contains a disulfide linkage in the center of the triblock copolymer and two disulfides at block junctions. Figure 3a illustrates the reduction-responsive cleavage of the disulfide linkages in DL-ssABP to the corresponding thiols; HS-PLA-SH and POEOMA-SH. Aliquots of DL-ssABP were mixed with DTT (5 mol equivalent to disulfides) in DMF as a homogeneous solution under stirring and GPC was used to follow the cleavage of the disulfide linkages. As seen in Figure 3b, the GPC trace of DL-ssABP is shifted to low molecular weight region following treatment with DTT. Molecular weight decreased with incubation time and reached a plateau after 2 h, as a result of the cleavage of disulfide linkages at dual locations (Figure S2).

Aqueous Micellization and Disassembly of DL-ssABP. The resulting DL-ssABP is amphiphilic, consisting of a hydrophobic PLA middle block and hydrophilic POEOMA blocks. Its CMC was first determined using fluorescence spectroscopy with an NR probe.[76,77] A series of mixtures

dx.doi.org/10.1021/bm5008508 | Biomacromolecules 2014, 15, 3180−3189

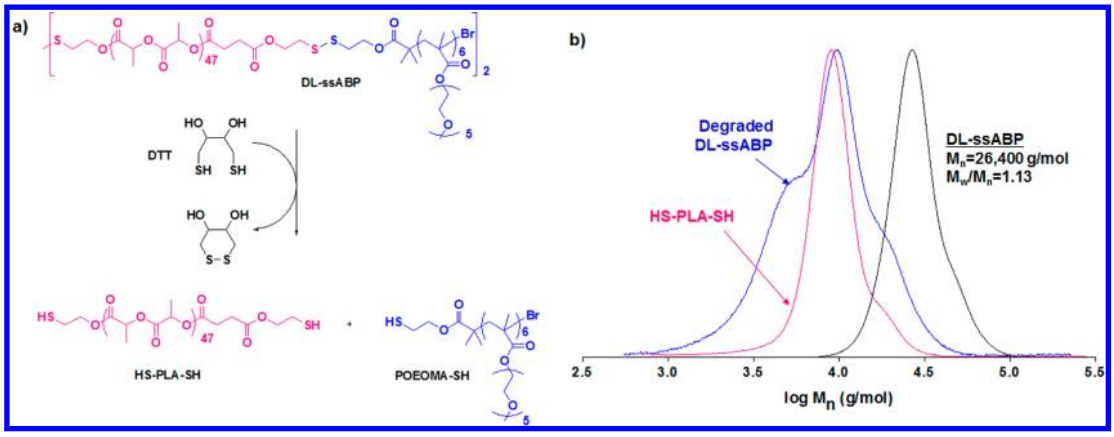

Figure 3. Reduction-responsive cleavage of disulfides of DL-ssABP in the presence of DTT (a) and GPC trace of degraded DL-ssABP after treatment with DTT in DMF, compared with DL-ssABP and HS-PLA-SH (b). Note that HS-PLA-SH is a degraded product of ss(PLA-ss-Br)$_2$ upon reductive cleavage of the disulfide linkages in DMF containing excess DTT for 2 h (the detailed procedure is given in the Supporting Information).

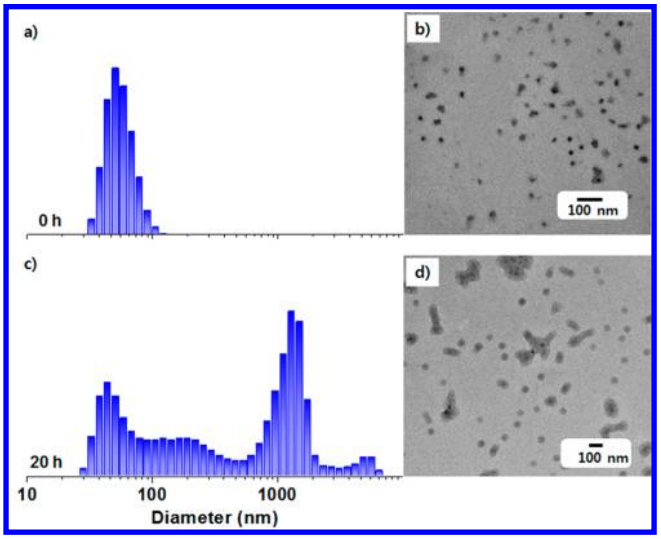

Figure 4. DLS diagrams (a,c) and TEM images (b,d) of DL-ssABP micelles before (a,b) and after (c,d) treatment with 10 mM GSH at 1.2 mg/mL.

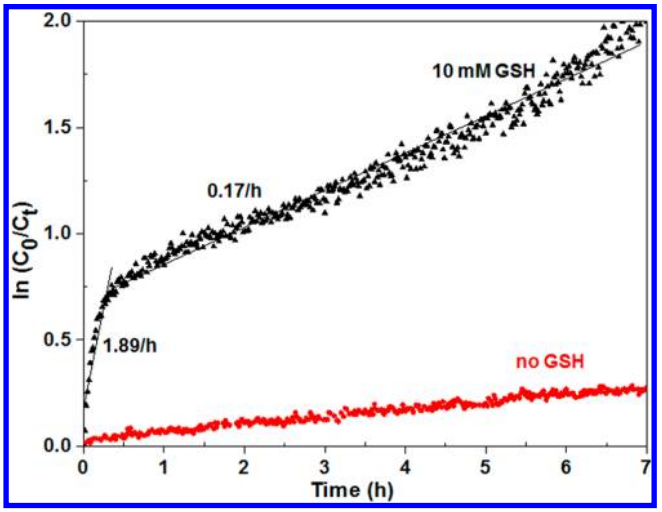

Figure 5. Enhanced release of DOX from DOX-loaded DL-ssABP micelles in the absence (control) and presence of 10 mM GSH. The apparent diffusion coefficients of DOX released from DOX-loaded micelles are calculated from the slopes obtained by fitting the data to a linear regression.

consisting of the same amount of NR in various concentration of DL-ssABP ranging from 5×10^{-6} to 0.4 mg/mL in aqueous solution were prepared. After the removal of THF by evaporation and excess NR by filtration (0.45 μm PES filter), their fluorescence spectra were recorded (Figure S3a). The method is based on the fact that the fluorescence intensity of NR increases when NR is entrapped in hydrophobic PLA core, while it is low in water due to low solubility of NR in water. From the linear regressions of fluorescence intensity at λ_{max} = 600 nm, the CMC of DL-ssABP was determined to be 43 μg/mL (Figure S3b).

At concentrations above the CMC, DL-ssABP self-assembles through aqueous micellization to form micellar aggregates consisting of hydrophobic PLA cores surrounded with hydrophilic POEOMA coronas. For example, aqueous self-assembled aggregates were prepared using a solvent evaporation method at a concentration of 1.2 mg/mL, and their size and morphology were examined using DLS and TEM. DLS results indicate a hydrodynamic diameter of ≈55 nm with a monomodal size distribution (Figure 4a). TEM images indicate an average diameter of 30.4 ± 6.5 nm with relative broad size distribution (Figure 4b), which is smaller than the size determined by DLS. The difference in micelle sizes between DLS and TEM can be attributed to the dehydrated state of the micelles.[78]

The self-assembled micelles of DL-ssABP are composed of disulfide linkages in the dual locations positioned in the PLA cores and PLA/POEOMA interfaces. These disulfide linkages can be cleaved in response to reductive reactions, causing destabilization (or disassembly) of micelles. As seen in Figure 4c and 4d, both DLS and TEM results indicate the increase in micelle size with multimodal distribution in the presence of 10 mM GSH (a cellular reducing agent) after 20 h. The occurrence of aggregation is attributed to both hydrophobicity of cleaved HS-PLA-SH chains and amphiphilicity of cleaved POEOMA-SH chains generated upon the cleavage of disulfide linkages in the dual locations. Similar results of the occurrence of aggregation in the presence of reducing agents has been reported for polyester-based block copolymer micelles having multiple disulfide linkages positioned in the main chains.[40]

Loading and GSH-Triggered DOX Release. The resulting DL-ssABP based micelles were evaluated for enhanced release of encapsulated anticancer drugs in the presence of

dx.doi.org/10.1021/bm5008508 | *Biomacromolecules* 2014, 15, 3180−3189

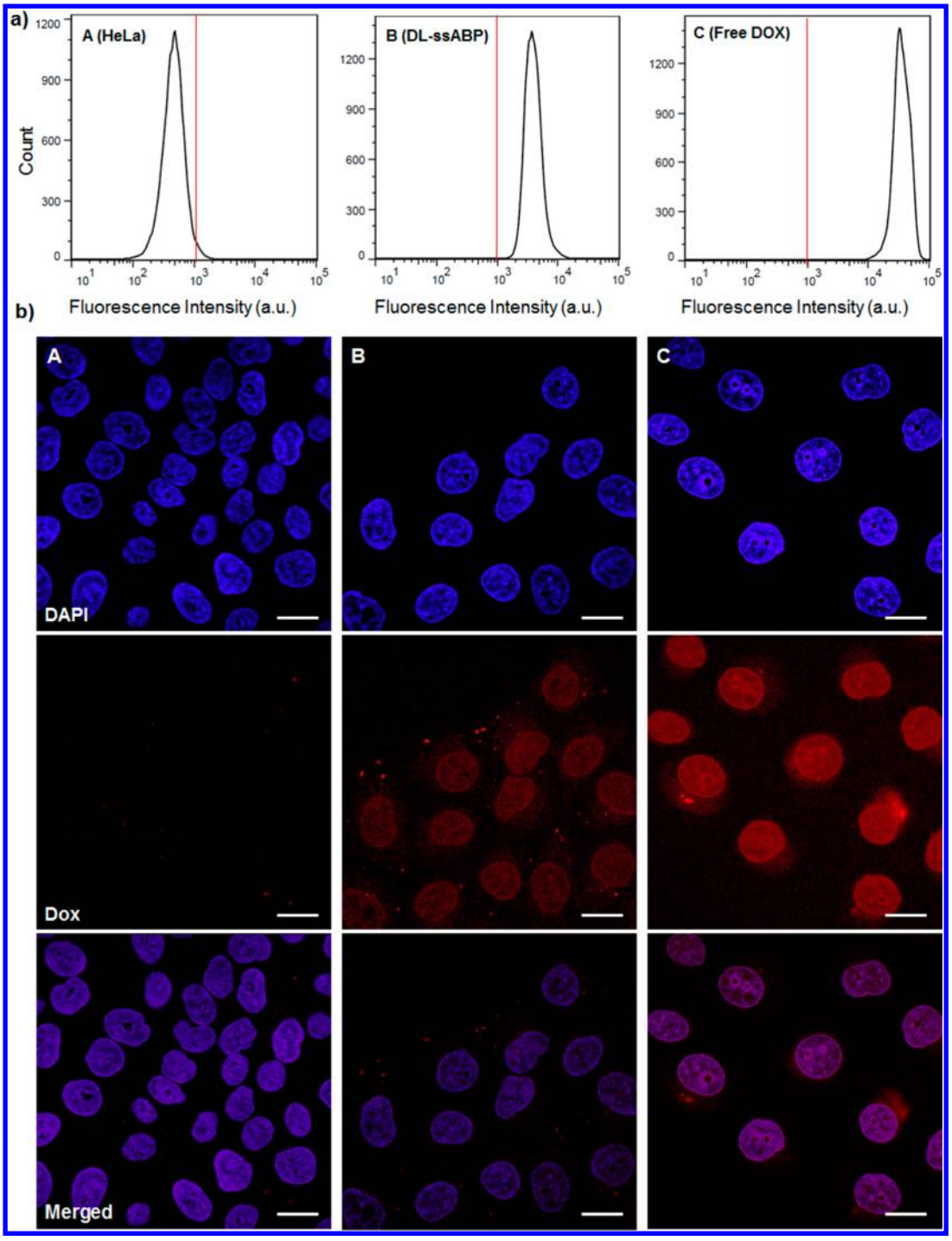

Figure 6. Flow cytometric histograms (a) and CLSM images (b) of HeLa cells only (A) and incubated with DOX-loaded DL-ssABP micelles (B), and free DOX (C) for 16 h. Scale bar = 20 μm.

GSH. To prepare DOX-loaded micelles using a dialysis method, an aliquot of DOX ($NH_3^+Cl^-$ forms) was pretreated with Et_3N (3 mol equivalents) in DMF for deprotonation in order to increase its solubility in the hydrophobic micellar core. The organic mixture was transferred into a dialysis tubing and then dialyzed over water over 2 days to remove DMF and free (not encapsulated) DOX. Using UV/vis spectroscopy with the predetermined extinction coefficient of DOX = 12 400 M^{-1} cm^{-1} in a mixture of water/DMF = 1/5 v/v at λ = 497 nm,[68] the loading level of DOX was determined to be 2.2 ± 0.5 wt % at the initial ratio of DOX/polymer = 1/10 wt/wt.

Next, GSH-responsive release of DOX from DOX-loaded micelles was examined in the absence (control) and presence of 10 mM GSH in PBS solution. DOX can diffuse through the dialysis tubing after GSH-triggered release from DOX-loaded micelles. Its UV absorbance accumulated in the outer solution was recorded using a UV spectrometer equipped with an external probe at λ = 497 nm. As compared in Figure 5, the DOX release from DL-ssABP micelles was faster in the presence of 10 mM GSH than without GSH. For example, within 5 h, the release reached >80% in the presence of 10 mM GSH, while <20% in the absence of GSH. Further, the apparent

dx.doi.org/10.1021/bm5008508 | *Biomacromolecules* 2014, 15, 3180−3189

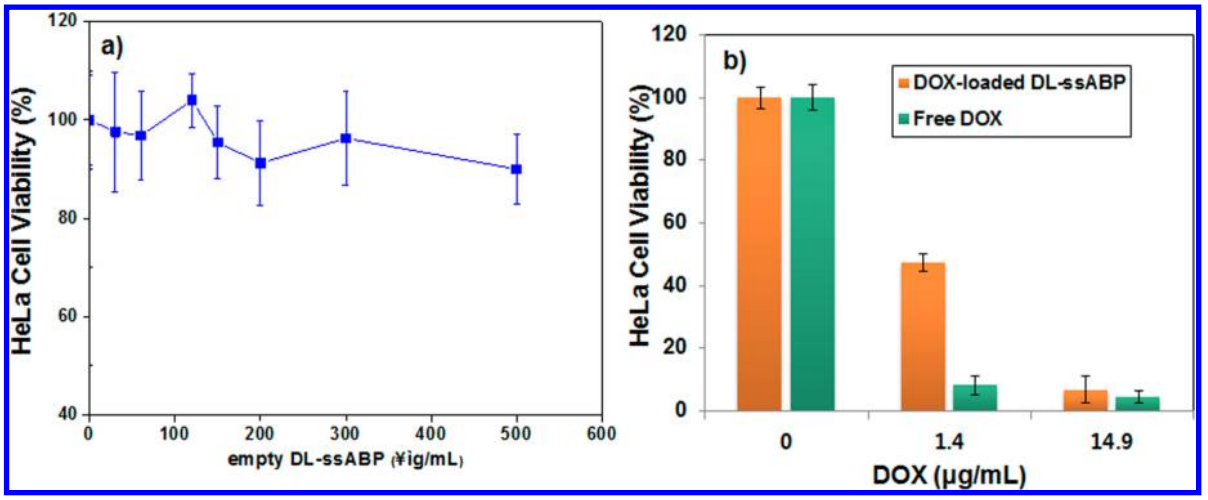

Figure 7. Viability of HeLa cells incubated with different amounts of empty (DOX-free) micelles (a) and free DOX and DOX-loaded micelles (b) for 48 h determined by MTT assay. Data are presented as the average ± standard deviation (n = 12).

diffusion coefficient of DOX from DL-ssABP micelles was calculated to be 1.89/h within 30 min, which is much larger than 0.17/h, showing an early burst release of encapsulated DOX (around 60%) in the presence of GSH. The enhanced and early burst release is presumably attributed to the reductive cleavage of disulfide linkages in dual locations as in micellar cores and at interfaces. In comparison with monocleavable micelles having single disulfides in the middle of triblock copolymers, the model release kinetics is significantly more rapid.[33,35,79]

Intracellular Release and Antitumor Activity. Given a promising results, the DL-ssABP-based micelles were evaluated as effective intracellular drug delivery nanocarriers. Intracellular trafficking of DOX from DOX-loaded DL-ssABP micelles were examined using flow cytometry and CLSM. Figure 6a shows the flow cytometric histogram of HeLa cells incubated with DOX-loaded micelles and free DOX. Note that the amount of free DOX was designed to be the same as that encapsulated in DOX-loaded micelles. Compared with HeLa cells only as a control, their histograms presented a noticeable shift in the direction of high fluorescence intensity. Figure 6b shows CLSM images of HeLa cells with and without DOX-loaded micelles and free DOX for 16 h. HeLa nuclei were stained with DAPI. Obviously, HeLa cells incubated with DOX-loaded DL-ssABP micelles displayed strong DOX fluorescence in their nuclei. These results from both flow cytometry and CLSM confirm that DOX-loaded DL-ssABP micelles are able to delivery and release DOX into the nuclei of cancer cells. Compared to the images from free DOX which is brighter, the images from DOX-loaded micelles suggest that GSH-responsive DOX release may delay an access to targeted nuclei. In biological systems, cellular GSH-OEt can penetrate cellular membranes and rapidly reach a high intracellular concentration of GSH.[80] Several reports investigated the pretreatment of cancer cells with GSH-OEt to enhance cellular GSH levels. Compared with no pretreatment, the intracellular DOX release results suggest that DOX could be released from DOX-loaded micelles after uptake.[37,43,56,58]

In vitro cytotoxicity of DOX-free (empty) and DOX-loaded micelles based on DL-ssABP was compared with free DOX as a control using a MTT colorimetric assay. As seen in Figure 7a, empty micelles exhibited >90% of HeLa cell viability, suggesting noncytotoxicity of DL-ssABP micelles at concentrations up to 500 μg/mL. In the presence of DOX-loaded micelles, however, the HeLa cell viability decreased with an increasing concentration of DOX-encapsulated micelles. For example, the viability was <50% at 1.4 μg/mL, which is comparative to or lower than the reported other block copolymer-based nanocarriers to HeLa cells.[37,50,55] It further decreased to <5% at 15 μg/mL.[81] This decrease in HeLa cell viability suggests the inhibition of cellular proliferation due to the effective and rapid release of DOX from DL-ssABP platform. This is a consequence from the degradation of dual-located disulfide linkages in response to intracellular GSH inside cancer cells. Compared with DOX-loaded micelles, the HeLa cell viability is lower in the presence of free DOX at the same concentrations. These results are consistent to those obtained from flow cytometry and CLSM described above.

CONCLUSION

Novel PLA-based DL-ssABPs having both a disulfide in the center of hydrophobic PLA block and two disulfides at PLA/hydrophilic POEOMA block junctions were synthesized by a combination of well-defined organic and polymeric syntheses including ROP, facile coupling reactions, and ATRP. The DL-ssABP and the precursors synthesized in each synthetic step, as well as the degraded products generated by the cleavage of the disulfides positioned in dual locations were well characterized with molecular composition by ^{1}H NMR and molecular weights by GPC. Above the CMC, 43 μg/mol, the DL-ssABP self-assembled to form colloidally stable micellar aggregates having disulfides in dual locations; in the hydrophobic core and at the PLA/POEOMA interface. The cleavage of dual-location disulfide linkages in response to the GSH cellular trigger shed POEOMA coronas from the PLA core as well as disintegrated the hydrophobic PLA core, causing destabilization of the micelles. Such a disassembly enabled early burst and then a sustained enhanced release of encapsulated anticancer drugs. These results, combined with intracellular release of anticancer drugs into HeLa cancer cells confirmed by CLSM, flow cytometry, and MTT viability, suggest that the dual location disulfide degradation strategy accelerated the release of encapsulated model drugs from micelles.

dx.doi.org/10.1021/bm5008508 | Biomacromolecules 2014, 15, 3180−3189

■ ASSOCIATED CONTENT

Supporting Information

Additional characterization plots. This material is available free of charge via the Internet at http://pubs.acs.org.

■ AUTHOR INFORMATION

Corresponding Author

*E-mail: john.oh@concordia.ca.

Notes

The authors declare no competing financial interest.

■ ACKNOWLEDGMENTS

This work is supported by an NSERC Discovery Grant and a Canada Research Chair (CRC) Award. J.K.O. is entitled Tier II CRC in Nanobioscience as well as a member of Centre Québécois sur les Matériaux Fonctionnels (CQMF) funded by FQRNT.

■ REFERENCES

(1) Nishiyama, N.; Kataoka, K. *Adv. Polym. Sci.* **2006**, *193*, 67−101.
(2) Mikhail, A. S.; Allen, C. *J. Controlled Release* **2009**, *138*, 214−223.
(3) Allen, C.; Maysinger, D.; Eisenberg, A. *Colloids Surf., B* **1999**, *16*, 3−27.
(4) Xiong, X.-B.; Falamarzian, A.; Garg, S. M.; Lavasanifar, A. *J. Controlled Release* **2011**, *155*, 248−261.
(5) Harada, A.; Kataoka, K. *Prog. Polym. Sci.* **2006**, *31*, 949−982.
(6) Bae, Y. H.; Park, K. *J. Controlled Release* **2011**, *153*, 198−205.
(7) Farokhzad, O. C.; Langer, R. *ACS Nano* **2009**, *3*, 16−20.
(8) Prokop, A.; Davidson, J. M. *J. Pharm. Sci.* **2008**, *97*, 3518−3590.
(9) Taurin, S.; Nehoff, H.; Greish, K. *J. Controlled Release* **2012**, *164*, 265−275.
(10) Zhang, L.; Li, Y.; Yu, J. C. *J. Mater. Chem. B* **2014**, *2*, 452−470.
(11) Nichols, J. W.; Bae, Y. H. *Nano Today* **2012**, *7*, 606−618.
(12) Bareford, L. M.; Swaan, P. W. *Adv. Drug Delivery Rev.* **2007**, *59*, 748−758.
(13) Conner, S. D.; Schmid, S. L. *Nature* **2003**, *422*, 37−44.
(14) Klinger, D.; Landfester, K. *Polymer* **2012**, *53*, 5209−5231.
(15) Rijcken, C. J. F.; Soga, O.; Hennink, W. E.; van Nostrum, C. F. *J. Controlled Release* **2007**, *120*, 131−148.
(16) Zhao, Y. *Macromolecules* **2012**, *45*, 3647−3657.
(17) Jackson, A. W.; Fulton, D. A. *Polym. Chem.* **2013**, *4*, 31−45.
(18) Alvarez-Lorenzo, C.; Concheiro, A. *Chem. Commun.* **2014**, *50*, 7743−7765.
(19) Gillies, E. R.; Jonsson, T. B.; Frechet, J. M. J. *J. Am. Chem. Soc.* **2004**, *126*, 11936−11943.
(20) Binauld, S.; Stenzel, M. H. *Chem. Commun.* **2013**, *49*, 2082−2102.
(21) Zhao, H.; Sterner, E. S.; Coughlin, E. B.; Theato, P. *Macromolecules* **2012**, *45*, 1723−1736.
(22) Sun, L.; Zhu, B.; Su, Y.; Dong, C.-M. *Polym. Chem.* **2014**, *5*, 1605−1613.
(23) Bertrand, O.; Poggi, E.; Gohy, J.-F.; Fustin, C.-A. *Macromolecules* **2014**, *47*, 183−190.
(24) Xiong, M.-H.; Bao, Y.; Du, X.-J.; Tan, Z.-B.; Jiang, Q.; Wang, H.-X.; Zhu, Y.-H.; Wang, J. *ACS Nano* **2013**, *7*, 10636−10645.
(25) Li, C.; Madsen, J.; Armes, S. P.; Lewis, A. L. *Angew. Chem., Int. Ed.* **2006**, *45*, 3510−3513.
(26) Tsarevsky, N. V.; Matyjaszewski, K. *Macromolecules* **2005**, *38*, 3087−3092.
(27) Russo, A.; DeGraff, W.; Friedman, N.; Mitchell, J. B. *Cancer Res.* **1986**, *46*, 2845−8.
(28) Saito, G.; Swanson, J. A.; Lee, K.-D. *Adv. Drug Delivery Rev.* **2003**, *55*, 199−215.
(29) Cheng, R.; Feng, F.; Meng, F.; Deng, C.; Feijen, J.; Zhong, Z. *J. Controlled Release* **2011**, *152*, 2−12.
(30) Wei, H.; Zhuo, R.-X.; Zhang, X.-Z. *Prog. Polym. Sci.* **2013**, *38*, 503−535.
(31) Huo, M.; Yuan, J.; Tao, L.; Wei, Y. *Polym. Chem.* **2014**, *5*, 1519−1528.
(32) Ding, M.; Li, J.; He, X.; Song, N.; Tan, H.; Zhang, Y.; Zhou, L.; Gu, Q.; Deng, H.; Fu, Q. *Adv. Mater.* **2012**, *24*, 3639−3645.
(33) Cunningham, A.; Oh, J. K. *Macromol. Rapid Commun.* **2013**, *34*, 163−168.
(34) Liu, D.-L.; Chang, X.; Dong, C.-M. *Chem. Commun.* **2013**, *49*, 1229−1231.
(35) Sun, L.; Liu, W.; Dong, C.-M. *Chem. Commun.* **2011**, *47*, 11282−11284.
(36) Jiang, X.; Zhang, M.; Li, S.; Shao, W.; Zhao, Y. *Chem. Commun.* **2012**, *48*, 9906−9908.
(37) Liu, J.; Pang, Y.; Huang, W.; Zhu, Z.; Zhu, X.; Zhou, Y.; Yan, D. *Biomacromolecules* **2011**, *12*, 2407−2415.
(38) Han, D.; Tong, X.; Zhao, Y. *Langmuir* **2012**, *28*, 2327−2331.
(39) Nelson-Mendez, A.; Aleksanian, S.; Oh, M.; Lim, H.-S.; Oh, J. K. *Soft Matter* **2011**, *7*, 7441−7452.
(40) Aleksanian, S.; Khorsand, B.; Schmidt, R.; Oh, J. K. *Polym. Chem.* **2012**, *3*, 2138−2147.
(41) Fan, H.; Huang, J.; Li, Y.; Yu, J.; Chen, J. *Polymer* **2010**, *51*, 5107−5114.
(42) Yu, S.; He, C.; Ding, J.; Cheng, Y.; Song, W.; Zhuang, X.; Chen, X. *Soft Matter* **2013**, *9*, 2637−2645.
(43) Khorsand, B.; Lapointe, G.; Brett, C.; Oh, J. K. *Biomacromolecules* **2013**, *14*, 2103−2111.
(44) Ryu, J.-H.; Roy, R.; Ventura, J.; Thayumanavan, S. *Langmuir* **2010**, *26*, 7086−7092.
(45) Yuan, L.; Liu, J.; Wen, J.; Zhao, H. *Langmuir* **2012**, *28*, 11232−11240.
(46) Zhang, Q.; Aleksanian, S.; Noh, S. M.; Oh, J. K. *Polym. Chem.* **2013**, *4*, 351−359.
(47) Bapat, A. P.; Ray, J. G.; Savin, D. A.; Sumerlin, B. S. *Macromolecules* **2013**, *46*, 2188−2198.
(48) Zhang, Z.; Yin, L.; Tu, C.; Song, Z.; Zhang, Y.; Xu, Y.; Tong, R.; Zhou, Q.; Ren, J.; Cheng, J. *ACS Macro Lett.* **2013**, *2*, 40−44.
(49) Chen, W.; Zheng, M.; Meng, F.; Cheng, R.; Deng, C.; Feijen, J.; Zhong, Z. *Biomacromolecules* **2013**, *14*, 1214−1222.
(50) Wei, R.; Cheng, L.; Zheng, M.; Cheng, R.; Meng, F.; Deng, C.; Zhong, Z. *Biomacromolecules* **2012**, *13*, 2429−2438.
(51) Jia, Z.; Wong, L.; Davis, T. P.; Bulmus, V. *Biomacromolecules* **2008**, *9*, 3106−3113.
(52) Ryu, J.-H.; Chacko, R. T.; Jiwpanich, S.; Bickerton, S.; Babu, R. P.; Thayumanavan, S. *J. Am. Chem. Soc.* **2010**, *132*, 17227−17235.
(53) Li, Y.-L.; Zhu, L.; Liu, Z.; Cheng, R.; Meng, F.; Cui, J.-H.; Ji, S.-J.; Zhong, Z. *Angew. Chem., Int. Ed.* **2009**, *48*, 9914−9918.
(54) Chan, N.; An, S. Y.; Yee, N.; Oh, J. K. *Macromol. Rapid Commun.* **2014**, *35*, 752−757.
(55) Liu, J.; Pang, Y.; Huang, W.; Huang, X.; Meng, L.; Zhu, X.; Zhou, Y.; Yan, D. *Biomacromolecules* **2011**, *12*, 1567−1577.
(56) Tang, L.-Y.; Wang, Y.-C.; Li, Y.; Du, J.-Z.; Wang, J. *Bioconjugate Chem.* **2009**, *20*, 1095−1099.
(57) Klaikherd, A.; Nagamani, C.; Thayumanavan, S. *J. Am. Chem. Soc.* **2009**, *131*, 4830−4838.
(58) Wen, H.-Y.; Dong, H.-Q.; Xie, W.-j.; Li, Y.-Y.; Wang, K.; Pauletti, G. M.; Shi, D.-L. *Chem. Commun.* **2011**, *47*, 3550−3552.
(59) Sun, H.; Guo, B.; Li, X.; Cheng, R.; Meng, F.; Liu, H.; Zhong, Z. *Biomacromolecules* **2010**, *11*, 848−854.
(60) Khorsand Sourkohi, B.; Cunningham, A.; Zhang, Q.; Oh, J. K. *Biomacromolecules* **2011**, *12*, 3819−3825.
(61) Zhang, Q.; Ko, N. R.; Oh, J. K. *RSC Adv.* **2012**, *2*, 8079−8086.
(62) Yuan, W.; Zou, H.; Guo, W.; Shen, T.; Ren, J. *Polym. Chem.* **2013**, *4*, 2658−2661.
(63) Chen, W.; Zou, Y.; Meng, F.; Cheng, R.; Deng, C.; Feijen, J.; Zhong, Z. *Biomacromolecules* **2014**, *15*, 900−907.
(64) Xuan, J.; Han, D.; Xia, H.; Zhao, Y. *Langmuir* **2014**, *30*, 410−417.
(65) Tong, R.; Lu, X.; Xia, H. *Chem. Commun.* **2014**, *50*, 3575−3578.

(66) Jia, L.; Cui, D.; Bignon, J.; Di Cicco, A.; Wdzieczak-Bakala, J.; Liu, J.; Li, M.-H. *Biomacromolecules* **2014**, *15*, 2206−2217.
(67) Yuan, W.; Shen, T.; Wang, J.; Zou, H. *Polym. Chem.* **2014**, *5*, 3968−3971.
(68) Chan, N.; An, S. Y.; Oh, J. K. *Polym. Chem.* **2014**, *5*, 1637−1649.
(69) Chan, N.; Khorsand, B.; Aleksanian, S.; Oh, J. K. *Chem. Commun.* **2013**, *49*, 7534−7536.
(70) Penczek, S.; Cypryk, M.; Duda, A.; Kubisa, P.; Slomkowski, S. *Prog. Polym. Sci.* **2007**, *32*, 247−282.
(71) Uhrich, K. E.; Cannizzaro, S. M.; Langer, R. S.; Shakesheff, K. M. *Chem. Rev.* **1999**, *99*, 3181−3198.
(72) Dechy-Cabaret, O.; Martin-Vaca, B.; Bourissou, D. *Chem. Rev.* **2004**, *104*, 6147−6176.
(73) Ko, N. R.; Yao, K.; Tang, C.; Oh, J. K. *J. Polym. Sci., Part A: Polym. Chem.* **2013**, *51*, 3071−3080.
(74) Matyjaszewski, K.; Xia, J. *Chem. Rev.* **2001**, *101*, 2921−2990.
(75) Kamigaito, M.; Ando, T.; Sawamoto, M. *Chem. Rev.* **2001**, *101*, 3689−3745.
(76) Goodwin, A. P.; Mynar, J. L.; Ma, Y.; Fleming, G. R.; Frechet, J. M. J. *J. Am. Chem. Soc.* **2005**, *127*, 9952−9953.
(77) Jiang, J.; Tong, X.; Morris, D.; Zhao, Y. *Macromolecules* **2006**, *39*, 4633−4640.
(78) Huynh, V.-T.; de Souza, P.; Stenzel, M. H. *Macromolecules* **2011**, *44*, 7888−7900.
(79) Li, S.; Ye, C.; Zhao, G.; Zhang, M.; Zhao, Y. *J. Polym. Sci., Part A Polym. Chem.* **2012**, *50*, 3135−3148.
(80) Hong, R.; Han, G.; Fernandez, J. M.; Kim, B.-j.; Forbes, N. S.; Rotello, V. M. *J. Am. Chem. Soc.* **2006**, *128*, 1078−1079.
(81) Jin, Y.; Song, L.; Su, Y.; Zhu, L.; Pang, Y.; Qiu, F.; Tong, G.; Yan, D.; Zhu, B.; Zhu, X. *Biomacromolecules* **2011**, *12*, 3460−3468.

Supporting Information

Glutathione-triggered disassembly of dual disulfide located degradable nanocarriers of polylactide-based block copolymers for rapid drug release

Na Re Ko and Jung Kwon Oh*

Department of Chemistry and Biochemistry and Center for Nanoscience Research, Concordia University, Montreal, Quebec, Canada H4B 1R6

Reductive cleavage of disulfide linkages of ss(PLA-ss-Br)$_2$ in DMF. An aliquot of the dried, purified ss(PLA-ss-Br)$_2$ (10 mg) was mixed with excess DTT (5 mole equivalent to disulfides) in DMF (10 mL) under stirring at room temperature. Aliquots were taken periodically to analyze molecular weight distribution of degraded products using GPC.

Figure S1. GPC traces of DL-ssABP, compared with ss(PLA-OH)$_2$ precursor.

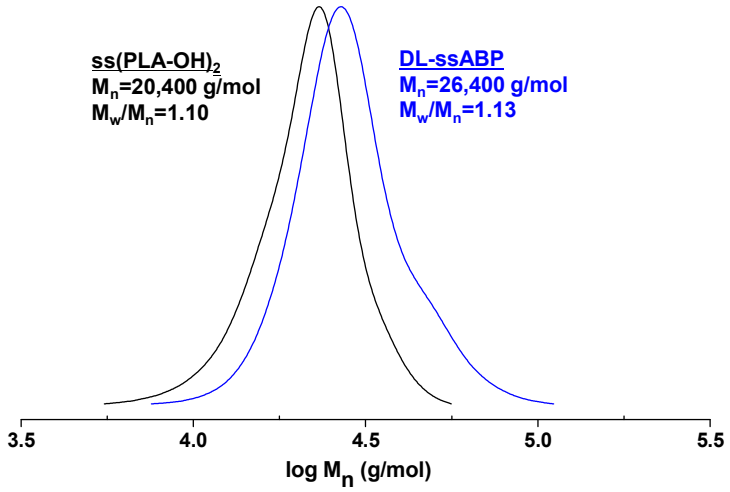

Figure S2. Evolution of molecular weights of DL-ssABP mixed with DTT (5 mole equivalents to disulfide linkages) over incubation time.

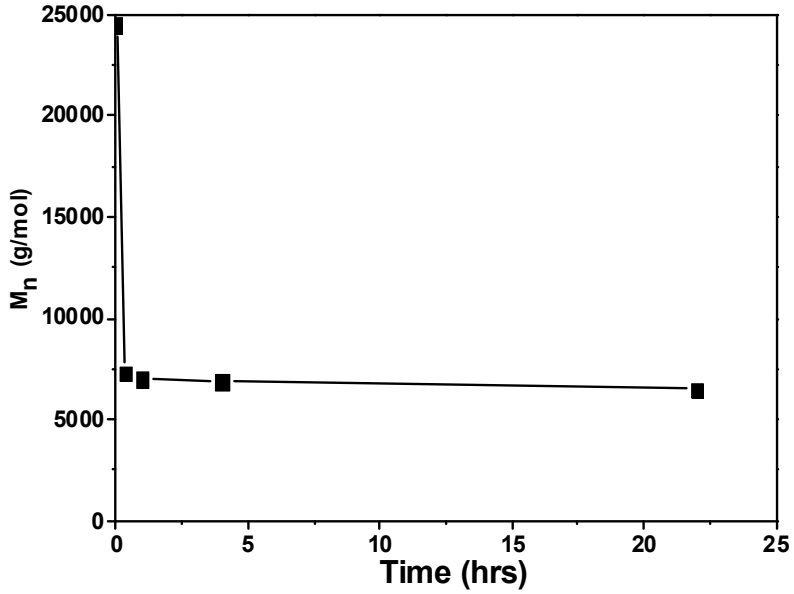

Figure S3. Evolution of fluorescence spectra of NR (a) and fluorescence intensity at 600 nm over concentration of DL-ssABP to determine CMC.